

Dihydro-Cucurbitacin-E; a Secondary Metabolite of *Curvularia lunata*'s Biotransformation as a Promising cPLA-2 and sPLA-2 Inhibitor in B[a]P-Induced Lung Toxicity



Mahmoud Abd El-Mongy¹, Mohammed Abdalla Hussein^{2,*}, Fotna Magdy Embabi³, Tamer Roshdy⁴ and Ahmed Salah⁴

¹Department of Microbial Biotechnology, Genetic Engineering and Biotechnology Research Institute, University of Sadat City, Egypt

²Department of Biotechnology, Faculty of Applied Health Sciences, October 6 University, Sixth of October City, Egypt

³Department of Medical Laboratories, Faculty of Applied Medical Sciences, October 6 University, Sixth of October City, Egypt

⁴Department of Molecular Biology, Genetic Engineering and Biotechnology Research Institute, University of Sadat City, Egypt

Abstract:

Background: Lung cancer is the most common cause of mortality, and its prevalence is rising quickly, making it a major global health concern. Numerous studies have indicated that benzo(a)pyrene [B[a]P] in cigarette smoke is the main cause of lung toxicity.

Objective: The study's goal was to apply *Curvularia lunata* NRRL 2178 in biotransformation cucurbitacin-E-glucoside to dihydro-cucurbitacin-E (DHCE). We characterized the isolated DHCE using ¹H-NMR and ¹³C-NMR spectra. We extended our study to evaluate the cancer activity of DHCE against A-549 cells *in vitro*, as well as its lung protective activity against B[a]P-induced lung toxicity.

Methods: We incubated *Curvularia lunata* NRRL 2178 with cucurbitacin-E-glucoside DHCE for 14 days. We isolated and characterized the obtained metabolite, DHCE, using ¹H-NMR and ¹³C-NMR techniques. We also evaluated the IC₅₀ of the isolated DHCE against A-549 cells. On the other hand, we conducted *in vivo* studies to assess its lung protective effect against B[a]P-induced toxicity in mice.

Results: The results of the ¹H-NMR and ¹³C-NMR experiments showed that the metabolite, DHCE, was found because it lacked two trans-olefinic protons (23 and 24) and the hydrogen atoms of the glucose moiety in the cucurbitacin-E-glucoside skeleton structure. The IC₅₀ value of DHCE against A-549 cells is 38.87 µg/mL, respectively. The LD₅₀ of DHCE was 930 mg/kg b.w. Giving DHCE (18.6 and 46.5 mg/kg b.w.) orally to mice that had been given B[a]P (20 mg/kg b.w.) every day for 30 days made their plasma total cholesterol (TC), triglycerides (TG), and high density lipoprotein-c (HDL-C) levels much better, as well as their lung reduced glutathione (GSH), catalase (CAT), glutathione peroxidase (GPx), and malondialdehyde (MDA) levels, compared to mice that had been given B[a]P. On the other hand, oral administration of DHCE enhanced plasma interleukin-6 (IL-6) and nuclear factor (NF)-κB, as well as matrix metalloproteinases-2 (MMP-2) and MMP-12, in the lung of treated mice. On the other hand, administering DHCE to lung mice treated with B[a]P reduced the activity of crucial genes linked to lung inflammation, specifically cytosolic (cPLA2) and Secretory Phospholipase A2 (sPLA2). Furthermore, DHCE nearly normalized these effects in lung histoarchitecture.

Conclusion: The obtained biochemical, molecular biology, and histological results proved the lung protective activity of *Curvularia lunata* metabolite (DHCE) against B[a]P-induced lung toxicity in mice.

Keywords: *Curvularia lunata*, B[a]P, Lung, Cucurbitacin-E, Biotransformation, B[a]P, Cytokines, Lung cancer.

© 2024 The Author(s). Published by Bentham Open.

This is an open access article distributed under the terms of the Creative Commons Attribution 4.0 International Public License (CC-BY 4.0), a copy of which is available at: <https://creativecommons.org/licenses/by/4.0/legalcode>. This license permits unrestricted use, distribution, and reproduction in any medium, provided the original author and source are credited.



Received: May 13, 2024
Revised: August 06, 2024
Accepted: August 15, 2024
Published: September 11, 2024



Send Orders for Reprints to
reprints@benthamscience.net

*Address correspondence to this author at the Department of Biotechnology, Faculty of Applied Health Sciences, October 6 University, Sixth of October City, Egypt; E-mail: prof.husseinma@o6u.edu.eg

Cite as: Abd El-Mongy M, Hussein M, Embabi F, Roshdy T, Salah A. Dihydro-Cucurbitacin-E; a Secondary Metabolite of *Curvularia lunata*'s Biotransformation as a Promising cPLA-2 and sPLA-2 Inhibitor in B[a]P-Induced Lung Toxicity. Open Microbiol J, 2024; 18: e18742858320564. <http://dx.doi.org/10.2174/0118742858320564240830110955>

1. INTRODUCTION

Lung cancer causes an alarming number of global fatalities [1]. The International Agency for Research on Cancer's (IARC) GLOBOCAN 2020 predicts that lung cancer will cause the deaths of approximately 1.8 million individuals (18%) in 2020 [2]. Benzo[a]pyrene (B[a]P) is an aromatic polycyclic hydrocarbon (PAH) that accounts for 20 to 70% of total tobacco smoke [3]. Incomplete organic material combustion generates benzo[a]pyrene through ingestion and inhalation. Activated cytochrome P450 sequentially transforms B[a]P into the carcinogenic epoxide benzo[a]pyrene after metabolic production [4].

World Health Organization (WHO) standards predict that chemoprevention, an alternative method, will impede the carcinogenesis process through the use of chemoprevention substances [5-12]. Chemoprevention is a plausible pharmacological preventive method that involves the use of one or more bioactive compounds, either synthetic or naturally occurring [12-25]. Biotransformation is the most common chemical reaction that changes the biological activity of target compounds [26]. When the glucose moiety is removed from cucurbitacin-E-glucose, CE, being less polar than the glycosylated form, may have improved bioavailability [27]. This structural change affects its solubility, cellular uptake, and interactions with target proteins. CE can more easily cross cell membranes and reach its intracellular targets. Moreover, reduction of the double bond between C23 and C24 in CE may affect the obtained overall conformation, stability, and binding affinity to relevant cellular targets [28, 29]. These changes could influence its ability to modulate signaling pathways involved in cancer progression.

Several fungi, including *Curvularia lunata* NRRL 2178, have been selected for our study to be applied in the hydroxylation reaction of steroids [29], whereas oxidation of the hydroxyl group to the corresponding keto function [30] is not a common biotransformation. Reports indicate that *C. lunata* breaks down the side chains of ecdysteroids, producing poststerone and rubrosterone [31].

Our study aimed to bio-transform cucurbitacin E glucoside by *C. lunata* NRRL 2178, evaluate the anticancer activity of the isolated dihydro-cucurbitacin (DHCE) metabolite against A-549 cells *in vitro*, and estimate its lung protective activity of, against B[a]P-induced lung toxicity in mice.

2. MATERIALS AND METHODS

All the chemicals used in this study were obtained from HiMedia Laboratories Pvt. Ltd. (Mumbai, India), Sigma Aldrich Chemical Co. All the chemicals used in this study were of analytical grade. Cucurbitacin-E-glucoside (98%) was obtained from Sigma-Aldrich (St. Louis, MO, USA). A549 cells are an epithelial cell line that was sourced from American Type Cell Culture (ATCC, USA, CAT: CRM-CCL-185), derived from human lung carcinoma.

The cells were maintained in Dulbecco's modified Eagle's medium (DMEM, Gibco, Gaithersburg, MD, USA) containing 10% (v/v) fetal bovine serum (FBS) and 5% horse serum, supplemented with penicillin/streptomycin (all from Gibco). We obtained the culture of *Curvularia lunata* NRRL 2178 from the Microbial Inoculants Center at Ain Shams University in Egypt and cultivated it using the conventional two-stage fermentation methodology [9].

HPLC System: Hewlett Packard 1100; Degasser: G1322A; Quaternary Pump: G1311; Auto Sampler: G1313A; Column Thermostat: G1316A; Variable Wavelength Detector: G1314A; Column: ODS C18, 25 cm x 4.6 mm, 5 μ m; Mobile Phase: Methanol; Flow Rate: 0.5 ml/min.; Detection Wavelength: 275 nm (determined using a UV-Visible Shimadzu spectrophotometer).

An electrothermal apparatus determined the melting point, and an uncorrected Jasco DIP-370 digital polarimeter recorded it. IR spectra recorded in KBr using the PerkinElmer FT-IR Spectrum BX spectro- photometer. ^1H and ^{13}C NMR were measured at 400 and 100 MHz, respectively, using a Bruker AVANCE 400 spectrometer. The unaffected solvent signal at μ 8.71 for the ^1H -NMR spectrum and μ 149.90 for the ^{13}C -NMR spectrum was used as a reference for the pyridine-d5 spectrum.

2.1. Biotransformation of Cucurbitacin-E-Glucoside

Several fungi, including *Curvularia lunata* NRRL 2178, have been selected for our study to be applied in the hydroxylation reaction of steroids. Potato dextrose agar was used to preserve the stock culture of *C. lunata* NRRL 2178. *C. lunata*, recently cultivated on agar, was transferred into 250-mL Erlenmeyer flasks containing 100 mL of liquid medium composed of 0.1% peptone, 0.1% yeast extract, 0.1% beef extract, and 0.5% glucose [28]. Each flask was cultivated at room temperature for 72 hours, then added a solution of cucurbitacin-E-glucoside (10 mg diluted in 100 mL DMSO and 5 mL Tween 80) and

extended the incubation for 14 to 17 days. Culture control consisted of a fermentation blank in which *C. lunata* was grown under identical conditions but without a cucurbitacin-E-glucoside substrate. Cucurbitacin-E-glucoside (28×10 mg) was fed to *C. lunata* in Erlenmeyer flasks (28×250 ml), each containing 100 ml of the same medium outlined above. After 14 days, the culture was filtered, and the mycelium was washed with nBuOH. Subject the crude products (450 mg) to column chromatography. Use a solvent system of dichloromethane (CH₂Cl₂) and methanol (MeOH) in a 92:8 ratio for elution. Isolate CE and DHCE with a yield of 281 mg and 170 mg, respectively.

The broth was extracted with n-BuOH, washed with H₂O, and the solvent evaporated under reduced pressure. The crude products (450 mg) were subjected to column chromatography eluting with CH₂Cl₂-MeOH (92:8) to give CE (281 mg, 62.44%, T_R 15.45) and DHCE (170 mg, 37.77%, T_R 27.32).

2.2. Determination of DHCE Cytotoxicity against A549 Cells

To determine the cytotoxic effect of DHCE, the methyl thiazolyl tetrazolium (MTT) cell viability assay was done using 96-well plates. A549 cells were seeded at 1×10⁴ cells/well. After 24 hours, or until a confluent monolayer was achieved, cells were treated with DHCE at different concentrations (0, 0.8, 1.6, 3.125, 6.250, 12.5, 25, 50, and 100 µg/mL). Cell viability was measured after 72 hours of treatment by removing the medium, adding 28 µL of a 2 mg/mL solution of MTT stain, and incubating the cells for 3 hours at 37 °C. After removing the MTT solution, the crystals remaining in the wells were solubilized by the addition of 130 µL of DMSO 2.5%, followed by 37 °C in a CO₂ incubator (Cypress Diagnostics, Belgium) at 5% CO₂ for 15 min with shaking [32]. The absorbency was determined on a microplate reader (BioTek, USA) at 492 nm, and the assay was performed in triplicate. The inhibition rate of cell growth (the percentage of cytotoxicity) was calculated using the following equation:

$$\text{Cytotoxicity} = [A-B/A] \times 100\%$$

Where A is the optical density of the control and B is the optical density of the samples.

2.3. Determine the LD50 of DHCE

Initial trials were conducted on cohorts of four mice. Various dosages of DHCE were administered to determine the lethal dose range, resulting in 0% and 100% mortality in animals. We measured the LD50 by administering DHCE orally at dosages ranging from 300 to 1800 mg/kg body weight. We counted the rate of animal death in separate groups during the 4-day observation period. With the increase in dose, the death rate also gradually rose. The LD₅₀ was determined by applying the Abal *et al.* formula as follows [33]:

$$LD_{50} = D_m - \left[\frac{\sum (Z \cdot d)}{n} \right]$$

D_m = The largest that kill all animals.

Σ = The sum of (z x d).

Z = Mean of dead animals between 2 successive groups.

d = the constant factor between two successive doses.

n = number of animals in each group.

2.4. Experimental Animals

The study was conducted following the setting established by the Faculty of Applied Health Science Technology, October 6 University, Egypt. 30 male albino mice weighing 35 ± 2.5 grams were acquired from the National Cancer Institute at Cairo University. Animals were housed in individual cages at a temperature of 22 ± 2 °C and a relative humidity of 60%. Each animal was provided with a regular diet of ad libitum during the experimental period.

2.5. Experimental Setup

This experiment was performed to examine the lung protective activity of DHCE against b[a]p-induced lung toxicity. For 30 days, the following were treatments for 6 groups of animals, each consisting of 6 mice (Table 1).

On the 31st day, blood was collected and centrifuged, and plasma was used fresh for estimation of plasma TC, TG, and HDL-c using commercially available kits (Asan and Youngdong Pharmaceutical Co., Korea) [36, 37]. Plasma IL-6 and NF-Kb were measured using ELISA kits from RayBiotech, Inc., USA, Quest Diagnostics Nichols Institute, San Juan Capistrano, California, and R&D Systems Inc., Minneapolis, MN, USA, respectively.

Table 1. Description of treatment groups.

| Groups | Treatment Description | Treatment Description |
|--------|-------------------------------------|---|
| I | Normal control | 3 mL of distilled water orally for 30 days |
| II | B[a]P (20 mg/kg b.w.) (Model group) | was given B[a]P orally in propylene glycol in a single daily dose for 30 days [34]. |
| III | B[a]P + DHCE (18.6 mg/kg.b.w.) | was treated with DHCE (18.6 mg/kg.b.w.) suspended in propylene glycol orally for 30 days. |
| IV | B[a]P + DHCE (46.5 mg/kg.b.w.) | was treated with DHCE (46.5 mg/kg.b.w.) suspended in propylene glycol orally for 30 days |
| V | B[a]P + Tamoxifen (2 mg/kg.b.w) | was treated with Tamoxifen (2 mg/kg.b.w) orally suspended in propylene glycol in a single weekly dose for 30 days [35]. |

Table 2. Primer sequences for real-time PCR.

| Gene | Primer's Sequence |
|--------------------------------|--|
| cPLA-2 | F:5'- CCTGATATGGAGAAAGATTGCC -3' R:5'- AGGGAACAGACCAACG-AGA -3' |
| sPLA-2 | F:5'-GACGACAGGAAAGGAAGCC-3' R:5'- TCCCTCTGCAGTGTATTGG-3' |
| GAPDH (a housekeeping gene) | F:5'- AACTTTGGCATTGTGGAAGG-3' R:5'- ACACATTGGGGTAGGAACA -3 |

Lungs were dissected out, and then lung samples were homogenized in a glass homogenizer (Universal Lab. Aid MPW-309, mechanika precyzyjna, Poland). The first portion was homogenized with ice-cold saline to create a 25% w/v homogenate. We produced three separate aliquots of the homogenate. The ELISA method was used to assess lung MMP-2 and MMP-12 (Abnova, Taipei City, Taiwan) in the first aliquot. The second aliquot was deproteinized with 12% (ice-cold) trichloroacetic acid and centrifuged at 1000 ×g, and the supernatant produced was used to quantify the amount of malondialdehyde (MDA) (MyBioscience, USA) [38]. The cytosolic portion of the lung was isolated by centrifuging the third portion of the homogenate at 10500 ×g for 15 minutes at 4 °C in a cooling ultracentrifuge. We assessed the levels of GPx, CAT, and GSH using the ZeptoMetrix diagnostic kit technique.

2.6. qRT-PCR Assays

Total RNA was collected from the second part of lung specimens using real-time quantitative PCR, and sections (10–15 mg) of recovered RNA were submitted to real-time PCR analysis using Sepasol-RNA1Super according to the manufacturer's instructions. RT-PCR was performed with 50ng of RNA template per reaction using the SensiFAST™ SYBR® Hi-ROX One-Step Kit (Meridian Bioscience Inc./Bioline; Memphis, TN, USA) in a 25µL reaction volume containing 70nM of specific primers in the Applied Biosystems 7500 Fast Real-Time PCR System (Foster City, CA, USA). The conditions of the reaction were pre-incubation at 50 °C in 2 minutes, followed by 10 min by 40 cycles of 95 °C in 15 s and 60 °C in 1 minute in 1 minute, respectively. The sequences of the primers are listed in Table 2.

2.7. Histological Assessment

The third section of lung specimens was dried in graded alcohol and embedded in paraffin after being fixed in a 10% neutral formalin solution. The fine slices (5µm thickness) were stained with hematoxylin & eosin (H&E) and mounted on glass slides for light microscopic inspection using Bancroft and Steven's approach [39, 40].

2.8. Statistical Analysis

All data was statistically assessed using the SPSS/20 program. The data were presented as mean ± SD (n = 6) and analyzed by one-way analysis of variance (ANOVA). P values less than 0.05 were considered statistically significant.

2.9. Ethical Declaration

The experiment received approval from the Ethics Committee of the Faculty of Applied Health Science and Technology (reference number 20221025). The animal research techniques were conducted according to the guidelines specified in the ninth edition of the Guide for the Care and Use of Laboratory Animals issued by the National Academy of Sciences, National Academies Press, Washington, D.C.

3. RESULTS

In the present study, cucurbitacin-E-glucoside was biotransformed by *C. lunata* (NRRL 2178). The isolated metabolites CE and DHCE were obtained as pale-yellow amorphous powders.

CE, the main metabolite, was isolated in 281 mg, yielding 62.44%. by CH₃OH-CHCl₃ as a crystallizing solvent, it showed MP 232 °C, ¹H-NMR, and ¹³C-NMR spectral data as follows. ¹H NMR (DMSO-d₆, 400 MHz): δ 0.926 (1H, s, H-18), 1.11 (3H, s, 19-Me), 1.202 (2 x 1H, s, H-26 and 27), 1.99 (2H, d, H-7), 2.127 (1H, overlapping signal, H-17), 2.176 (1H, s, H21), 2.28 (1H, obscured signal, H-23), 2.499 (1H, d, H-9), 2.5 (1H, d, J = 13.6 Hz, H-1), 4.759 (2 x 1H, s, H-28 and 29), 7.3-7.4 (d, 2H, CH=CH, J= 15.7, two trans-olefinic protons H 23 and 24) and absent of hydrogen atoms of glucose moiety.

¹³C NMR (CD₃OD, 100 MHz): δ 14.033 (C-15), 14.3 (C-32), 21.76 (C-20), 22.215 (C-4), 28.815 (C-5), 29.315 (C-6), 29.740 (C7), 31.027 (C-24), 31.413 (C-25), 38.221 (C-23), 38.947 (C-10), 39.504 (C-8), 39.782 (C-13), 40.016 (C-14), 41.78 (C-9), 42.34 (C-12), 62.347 (C-17), 69.45 (C-16), 105.33 (C-31), 120.914 (C-3), 127.857 (C-2), 129.380 (C-1), 174.915 (C-11), 183.45 (C-22), and absent of carbon atoms of glucose moiety.

DHCE, the second metabolite, was produced in (170 mg, 37.77%) yield as a pale-yellow amorphous powder with m.p. of 148-149 °C. ¹H- NMR (DMSO-d₆, 400 MHz): δ 0.84 (1H, s, H-18), 2.257 (1H, s, H-19), 1.22 (2× 1H, s, H-26&27), 2.08 (2H, d, H-7), 2.172 (1H, overlapping signal, H17), 2.393 (3H, s, 21-Me), 2.7 (1H, obscured signal, H-23), 3.336 (1H, d, H-9), 5.3 (1H, d, J = 13.6 Hz, H-1), 4.11 & 4.22 (2×1H, s, H-28&29) and absent of glucose moiety and olefinic protons H 23 and 24. ¹³C-NMR (CD₃OD, 100 MHz): δ 24.336 (C-15), 18.53 (C-32), 24.336 (C-20), 25.036 (C-4), 28.971 (C-5), 29.638 (C-6), 30.643 (C7), 38.5 (C-24), 38.916 (C-25), 39.752 (C-23), 40.195 (C-10), 42.933 (C-8), 48.705 (C-13), 61.736 (C-14), 68.759 (C-9), 71.305 (C-12), 78.334 (C-17), 79.852 (C-16), 109.64

(C-31), 120.625 (C-3), 124.644 (C-2), 126.743 (C-1), 152.848 (C-11), 172.761 (C-22), and absent of carbon atoms of glucose moiety.

3.1. IC₅₀ of DHCE

Mammalian cell lines: A-549 (human Lung carcinoma) cells were used as tumor cell lines. The cytotoxicity results of DHCE are shown in Table 3 and Figs. (1-2). IC₅₀ value

of DHCE against A-549 cells recorded 38.87 µg/mL.

3.2. LD₅₀ of DHCE in Mice

The results given in Table 4 show that oral administration of DHCE in doses of 300, 600, 900, 1200, 1500, and 1500 mg/k.g.b.w. resulted in mortalities of 1, 3, 5, 8, 9 and 10, respectively. The dose of DHCE that killed half of the mice (LD₅₀) was 930 mg/k.g b.w.

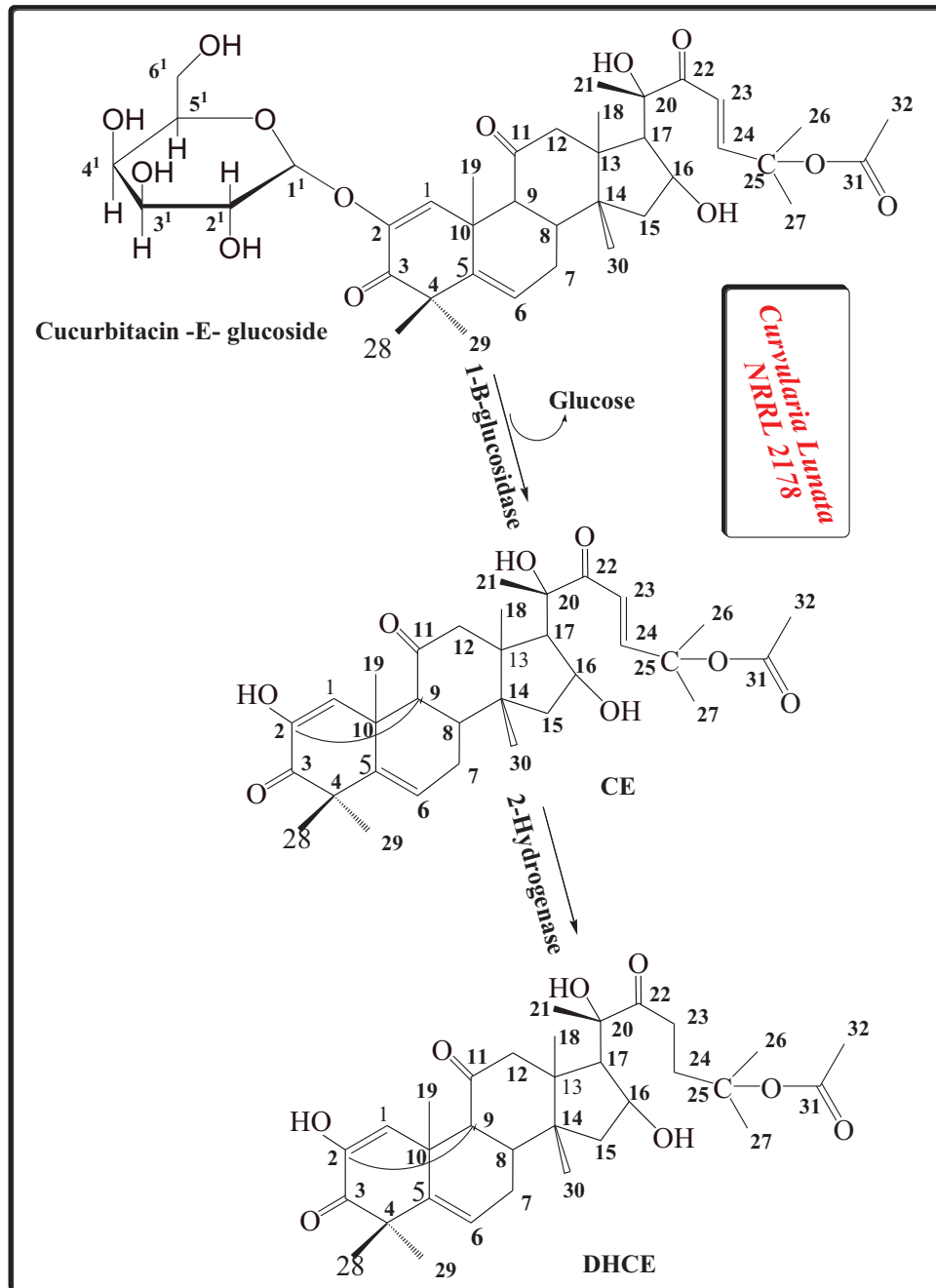


Fig. (1). Proposed pathway for the formation of cucurbitacin-E-β-D-glucoside metabolites by *Curvularia Lunata* NRRL 2178.

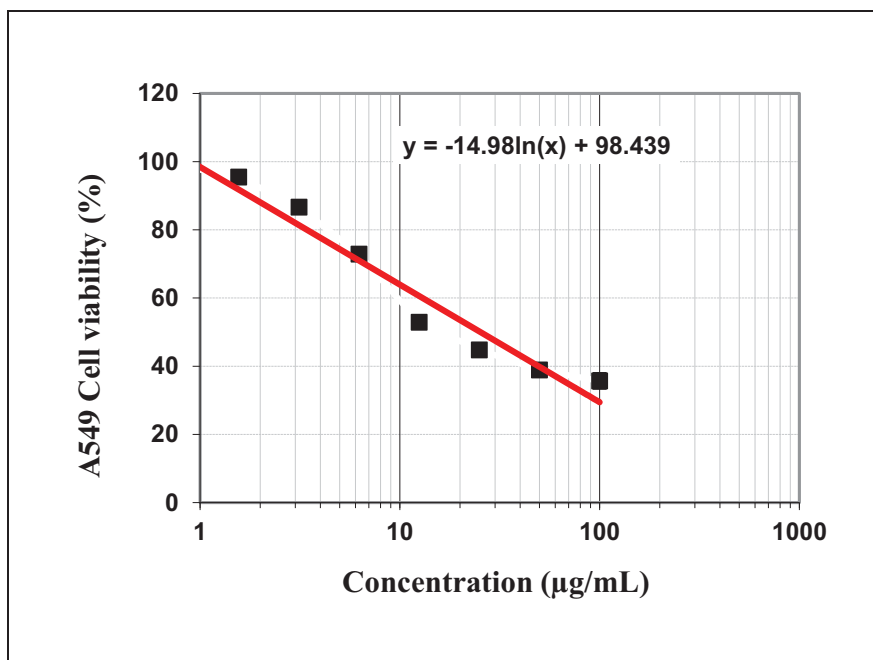


Fig. (2). IC₅₀ value of dihydro-cucurbitacin (DHCE) against A549 cells.

Table 3. IC₅₀ value of dihydro-cucurbitacin (DHCE) against A549 cell lines.

| DHCE conc. (µg/ml) | Mean of Viability % | The Mean of Inhibitory % | S.D. (±) |
|--------------------|---------------------|--------------------------|----------|
| 100 | 35.70 | 64.30 | 2.15 |
| 50 | 38.90 | 61.1 | 1.65 |
| 25 | 44.76 | 55.24 | 1.52 |
| 12.5 | 52.87 | 47.13 | 1.08 |
| 6.25 | 72.90 | 27.1 | 0.52 |
| 3.125 | 86.63 | 13.37 | 1.14 |
| 1.56 | 95.50 | 4.50 | 0.74 |
| 0.8 | 98.72 | 1.28 | 0.63 |
| 0 | 100 | 0 | 0 |
| IC ₅₀ | 38.87 ± 2.52 µg/ml | | |

Table 4. LD₅₀ of dihydro-cucurbitacin (DHCE) given orally in adult mice.

| Group Number | Dose (mg/kg) | No. of Animals/group | No. of Dead Animals | (Z) | (d) | (Z.d) |
|--------------|--------------|----------------------|---------------------|------|-----|-------|
| 1 | 300 | 10 | 1 | 2.0 | 300 | 600 |
| 2 | 600 | 10 | 3 | 4.00 | 300 | 1200 |
| 3 | 900 | 10 | 5 | 6.50 | 300 | 1950 |
| 4 | 1200 | 10 | 8 | 8.50 | 300 | 2250 |
| 5 | 1500 | 10 | 9 | 9.5 | 300 | 2700 |
| 6 | 1800 | 10 | 10 | 0 | 00 | 8700 |

Note:

$$LD_{50} = D_m - \left[\frac{\sum (Z \cdot d)}{n} \right]$$

$$LD_{50} = 1800 - \left[\frac{8700}{10} \right] = 930 \text{ mg/Kg.b.w.}$$

3.3. Effect of DHCE on TC, TG, and HDL-C in the Plasma of Treated Mice

Administration of B[a]P to normal mice showed a significant increase in plasma TC, TG, IL-6 and NF- κ B levels by 35.65, 68.05, 39.31, and 227.15%, respectively, as well as a significant decrease ($p < 0.05$) in plasma HDL-C by 42.81% when compared to normal mice (Table 5). However, compared to B[a]P-exposed mice, DHCE (18.6 mg/kg b.w.) treatment resulted in a considerable decrease in plasma TC, TG, IL-6 and NF- κ B by 21.80, 35.52, 12.76, and 42.28%, respectively, as well as a significant increase in plasma HDL-c by 126.25% ($p < 0.05$). Furthermore, the treatment of mice with DHCE (46.5 mg/kg b.w.) showed a significant depletion in plasma TC, TG, IL-6 and NF- κ B by 24.60, 35.20, 24.52, and 62.18%, respectively, as well as a significant increase in plasma HDL-c of 57.49% in comparison to B[a]P-treated mice ($p < 0.05$). However, treatment of mice with tamoxifen showed a significant decrease in plasma TC, TG and IL-6 by 15.51, 16.05, and 19.84%, respectively, as well as a non-significant change in plasma HDL-C and NF- κ B in comparison to B[a]P-treated mice.

3.4. Effect of Dihydro-cucurbitacin (DHCE) on GSH, CAT, GPx, and MDA in the Lung of Treated Mice

Lung GSH, CAT, and GPx levels were significantly decreased by 57.84, 62.36, and 78.18, respectively, as well as a significant increase in lung MDA levels by 69.41% in B[a]P-administered mice compared to the normal group (Table 6). On the other hand, when the experimental mice were treated with B[a]P and then administered DHCE (18.6 mg/kg b.w.), lung GSH, CAT, and GPx levels were significantly increased by 102.57, 74.20, and 227.08%, respectively, as well as MDA levels, which were decreased significantly by 17.26% ($p < 0.05$). Moreover, administration of DHCE (46.5 mg/kg.b.w.) significantly increased the levels of lung GSH, CAT, and GPx by 118.64, 155.11, and 318.75%, respectively, as well as decreased MDA levels by 34.11% compared to the B[a]P-exposed mice ($p < 0.05$). In addition, administration of tamoxifen non-significantly changed the levels of GSH, CAT, and MDA, as well as significantly decreased GPx levels by 18.75% compared to the B[a]P-administrated mice ($p < 0.05$).

Table 5. Effect of DHCE on TC, TG, HDL-C, IL-6, and NF- κ B in plasma of treated mice.

| No. | Groups | TC (mg/dl) | TG (mg/dl) | HDL-C (mg/dl) | IL-6 (pg/ml) | NF- κ B (pg/ml) |
|-------|---------------------------------|-------------------------|-------------------------|-----------------------|-------------------------|-------------------------|
| (I) | Normal control | 174.51 $\pm 12.45^a$ | 113.76 $\pm 6.19^a$ | 35.83 $\pm 2.13^c$ | 150.62 $\pm 14.20^a$ | 112.80 $\pm 8.99^a$ |
| (II) | B[a]P (20 mg/kg b.w.) | 236.74 $\pm 7.15^d$ | 191.17 $\pm 13.26^e$ | 20.49 $\pm 3.05^a$ | 209.83 $\pm 10.98^e$ | 369.03 $\pm 13.69^e$ |
| (III) | B[a]P + DHCE (18.6 mg/kg.b.w.) | 185.13 $\pm 14.62^b$ | 154.00 $\pm 8.67^c$ | 25.87 $\pm 2.03^b$ | 183.04 $\pm 15.10^c$ | 212.98 $\pm 14.76^c$ |
| (IV) | B[a]P + DHCE (46.5 mg/kg.b.w.) | 178.50 $\pm 9.05^a$ | 123.86 $\pm 6.00^b$ | 32.27 $\pm 2.86^c$ | 158.37 $\pm 12.75^b$ | 132.17 $\pm 11.49^b$ |
| (V) | B[a]P + Tamoxifen (2 mg/kg.b.w) | 200.02 $\pm 13.72^c$ | 160.48 $\pm 7.19^d$ | 18.76 $\pm 2.29^a$ | 251.47 $\pm 12.72^d$ | 397.84 $\pm 22.01^d$ |

Note: Values represent the mean \pm SE (n=6). Data shows mean \pm standard deviation of several observations within each treatment. Data followed by the same letter are not significantly different at $P \leq 0.05$.

Table 6. Effect of DHCE on GSH, CAT, GPx, and MDA in lungs of treated mice.

| No. | Groups | GSH (μ mol/mg protein) | CAT (U/mg protein) | Glutathione peroxidase (nmol NADPH/min/mg protein) | MDA (nmol/mg protein) |
|-------|---------------------------------|-----------------------------|-----------------------|--|------------------------|
| (I) | Normal control | 36.89 $\pm 3.22^c$ | 15.86 $\pm 1.63^d$ | 2.20 $\pm 0.29^e$ | 85.17 $\pm 7.74^a$ |
| (II) | B[a]P (20 mg/kg b.w.) | 15.55 $\pm 2.96^a$ | 5.97 $\pm 0.64^a$ | 0.48 $\pm 0.07^a$ | 144.29 $\pm 8.66^e$ |
| (III) | B[a]P + DHCE (18.6 mg/kg.b.w.) | 31.50 $\pm 3.37^b$ | 10.40 $\pm 1.10^b$ | 1.09 $\pm 0.16^c$ | 119.38 $\pm 9.29^c$ |
| (IV) | B[a]P + DHCE (46.5 mg/kg.b.w.) | 34.00 $\pm 2.41^b$ | 15.23 $\pm 1.22^c$ | 2.01 $\pm 0.23^d$ | 95.07 $\pm 7.66^b$ |
| (V) | B[a]P + Tamoxifen (2 mg/kg.b.w) | 16.24 $\pm 2.91^a$ | 6.01 $\pm 0.34^a$ | 0.39 $\pm 0.04^b$ | 162.40 $\pm 6.75^d$ |

Note: Values represent the mean \pm SE (n=6). Data shows mean \pm standard deviation of a number of observations within each treatment. Data followed by the same letter are not significantly different at $P \leq 0.05$.

3.5. Effect of DHCE on MMP-2 and MMP-12 in the Lung of Treated Mice

B[a]P-administrated mice dramatically increased their lung MMP-2 and MMP-12 by 72.36 and 74.94, respectively, compared to normal mice (Table 7). Administration of mice DHCE (18.6 mg/kg b.w.) significantly decreased the levels of MMP-2 and MMP-12 by 32.72 and 14.35 compared to B[a]P-administrated mice ($p < 0.05$). Moreover, giving DHCE (46.5 mg/kg.b.w.) to mice lowered their levels of MMP-2 and MMP-12 by 22.79 and 29.32 times compared to mice that had been exposed to B[a]P ($p < 0.05$). In addition, administration of tamoxifen significantly increased the levels of MMP-2 by 26.69%, respectively, compared to B[a]P-exposed mice ($p < 0.05$). Moreover, giving tamoxifen to mice that had been exposed to B[a]P did not significantly change the levels of MMP-12.

3.6. Effect of DHCE on Lung cPLA-2 and sPLA-2 Gene Expression in Treated Mice

Fig. (3) declares a significant increase of lung cPLA-2 and sPLA-2 gene expression by 902.97 and 659.40% in B[a]P-exposed mice as compared with normal mice. Administration of DHCE (18.6 mg/kg.b.w.) showed a significant decrease in the levels of cPLA-2 and sPLA-2 gene expression by 54.49 and 56.97%, respectively, as compared with B[a]P-exposed mice. Moreover, our results showed a significant decrease in cPLA-2 and sPLA-2 gene expression by 68.31 and 78.22%, respectively, in a group of mice treated with DHCE (46.5 mg/kg b.w.) as compared with B[a]P-exposed mice ($p < 0.05$). In addition, treatment of mice with tamoxifen showed a significant increase in cPLA-2 and sPLA-2 gene expression by 31.88% and 27.38%, respectively, as compared with B[a]P-administrated mice ($p < 0.05$).

Table 7. Effect of DHCE on MMP-2 and MMP-12 in lung of treated mice.

| No. | Groups | MMP-2 (ng/mg tissue) | MMP-12 (ng/mg tissue) |
|-------|---------------------------------|------------------------------|--------------------------------|
| (I) | Normal control | 48.35 ±4.91 ^a | 213.10 ±6.20 ^a |
| (II) | B[a]P (20 mg/kg b.w.) | 83.34 ±5.07 ^e | 372.8 ±16.55 ^e |
| (III) | B[a]P + DHCE (18.6 mg/kg.b.w.) | 56.07 ±4.43 ^b | 319.28 ±16.65 ^c |
| (IV) | B[a]P + DHCE (46.5 mg/kg.b.w.) | 64.35 ±2.84 ^c | 263.49 ±6.36 ^b |
| (V) | B[a]P + Tamoxifen (2 mg/kg.b.w) | 105.59 ±6.46 ^d | 386.14 ± 12.24 ^d |

Note: Values represent the mean ± SE (n=6). Data shows the mean ± standard deviation of several observations within each treatment. Data followed by the same letter are not significantly different at $P \leq 0.05$.

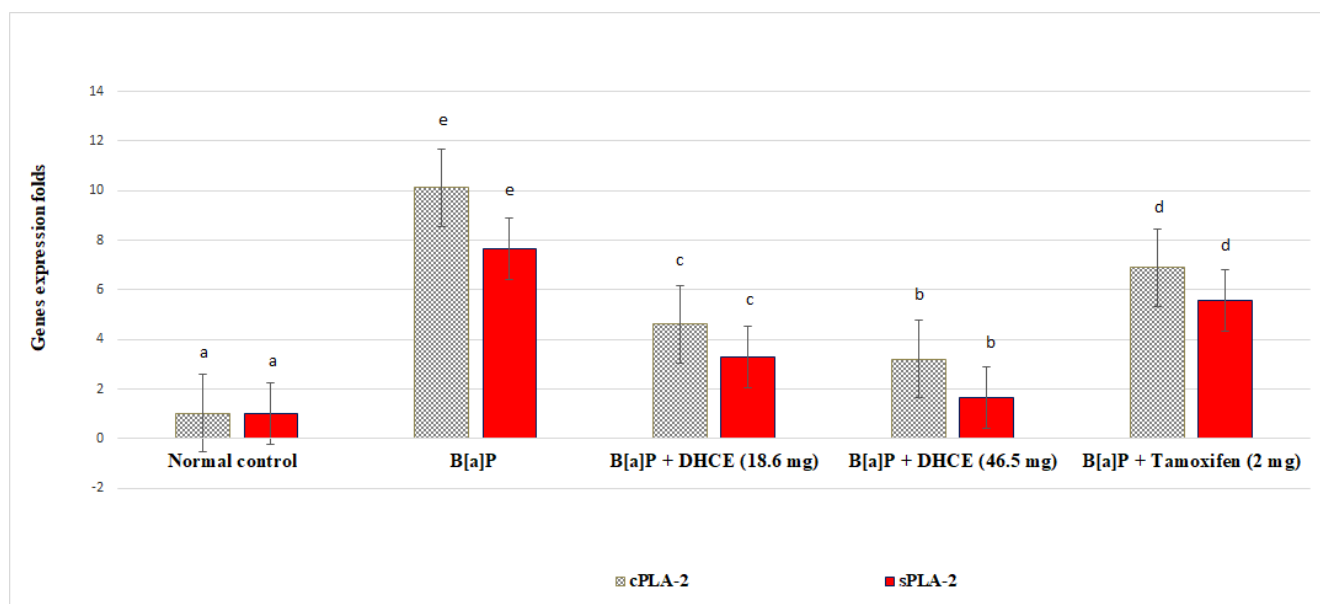


Fig. (3). Effect of dihydro-cucurbitacin (DHCE) on lung cPLA-2 and sPLA-2 gene expression in treated mice.

3.7. Histopathological Examination

Table 8 and Fig. (4a) show a photomicrograph of lung tissues (group I). Displaying a histological feature with no histopathological alterations. Lungs with typical alveoli (A) and inter-alveolar septa (arrow). The standard epithelial cell of the bronchi is readily visible (bold arrow).

Most pulmonary airways in group (II) B[a]P-administered mice suffered significant impairment. Numerous

alveoli looked deformed, with pronounced narrowing and collapse of numerous alveoli and expansion of adjacent alveoli (DA) and distended congested blood vessels (CO). Notable is the existence of a substantial mass of inflammatory cells (LI). There is a significant amount of red blood cell extravasation (EX). Most inter-alveolar septa were thickened (double-headed arrow), with areas of hemorrhage (H). Inter-alveolar septa exhibited vacuolation (wavy arrow) (Table 8 and Fig. 4b).

Table 8. Effect of dihydro-cucurbitacin (DHCE) on lung histopathological changes in treated mice.

| No. | Groups | Inflammation | Collapsed Alveoli | Widening Alveoli | Congestion | Thick Septa |
|-------|---------------------------------|--------------|-------------------|------------------|------------|-------------|
| (I) | Normal control | - | - | - | - | - |
| (II) | B[a]P (20 mg/kg b.w.) | +++ | +++ | +++ | +++ | +++ |
| (III) | B[a]P + DHCE (18.6 mg/kg.b.w.) | ++ | ++ | ++ | ++ | ++ |
| (IV) | B[a]P + DHCE (46.5 mg/kg.b.w.) | + | + | + | + | + |
| (V) | B[a]P + Tamoxifen (2 mg/kg.b.w) | ++ | ++ | ++ | + | + |

Note: (-) indicates normal, (+) indicates mild, (++) indicates moderate, (+++) indicates high.

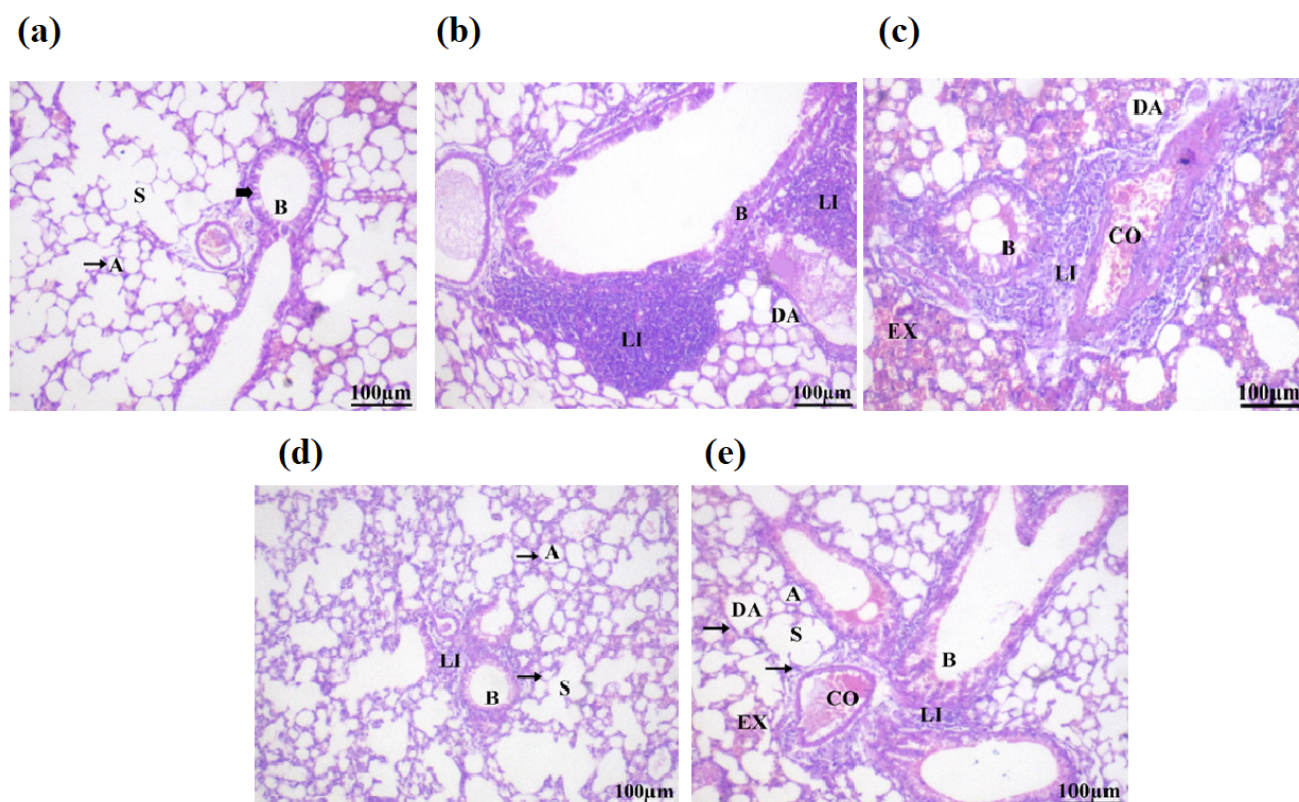


Fig. (4). Sections stained with hematoxylin and eosin (H&E; 200 X) histological examination of mice lung tissues of different groups compared to the control group. (a): Group I: Normal control; (b): Group II: Was administrate B[a]P (20 mg/kg b.w.); (c): Group III: B[a]P + DHCE (18.6 mg/kg.b.w.); (d): Group IV: B[a]P + DHCE (46.5 mg/kg.b.w.); (e): Group V: B[a]P + Tamoxifen (2 mg/kg.b.w).

Abbreviations: Alveolar lumina (A), pneumocyte-lined alveolar sacs (S), simple columnar epithelium-lined bronchioles (B), inter-alveolar septa (arrow), standard epithelial cell of the bronchi (bold arrow), a substantial mass of inflammatory cells (LI), expansion of adjacent alveoli (DA), distended congested blood vessels (CO), red blood cell extravasation (EX)

In group (III), B[a]P-exposed mice treated with DHCE (18.6 mg/kg b.w.), relative to the positive group, there was minor protection of the lungs. Significant inter-alveolar infiltration (LI) and many alveoli dilations (DA). The interalveolar septa appeared to have thickened, as indicated by the double-headed arrow. We found significant RBC extravasation (EX) in the alveolar cavities (Table 8 and Fig. 4c).

In group IV, a, B[a]P-exposed mice treated with DHCE (46.5 mg/kg b.w.), most regions of the lung sections displayed normal architecture with normally appearing alveoli (A) with thin inter-alveolar septa (arrows) and a moderate level of cellular infiltrations, indicating remarkable preservation as compared with the positive group. The bronchi exhibited their usual interior epithelium and bronchiolar anatomy. While the majority of interalveolar septa are thin (arrows), we still observed thickened septa (double-headed arrow). The configuration of alveolar sacs (S) and alveoli (A) is normal. Healthy simple columnar epithelium surrounds the bronchiole (B). Minorly congested blood vessels were observed (Table 8 and Fig. 4d).

In group (V), B[a]P-exposed mice treated with tamoxifen (2 mg/kg b.w.) demonstrated relative improvement in lung architecture but not full histological repair. It was seen that the bronchioles were dilated (B), there was moderate inflammatory cell infiltration in the moderately thickened septa (double-headed arrow) surrounding the alveoli and bronchioles, there were limited areas of smaller alveoli with enough dilatation (DA) of nearby alveoli, and some alveoli that looked normal (A) (Table 8 and Fig. 4e).

4. DISCUSSION

Biotransformation of cucurbitacin E glucosides by *C. lunata* NRRL 2178 and evaluation of their anticancer activity as well as estimation of the lung protective activity of the DHCE against benzo[a]pyrene-induced lung toxicity in mice were investigated in the present study.

Phase I clinical trials are currently investigating the antitumor effectiveness of several triterpenoids [41]. In addition, several reviews proved the microbial modification of terpenoids [42-44].

In the present study, *Curvularia lunata* efficiently metabolized curcbitacin-E-2-D-glucoside into two main metabolites: cucurbitacin-E and DHCE. We used solvent extraction to isolate the metabolites, followed by purification using column chromatography. We evaluated the metabolite yields using ¹H-NMR and C¹³-NMR spectroscopy.

The ¹H-NMR and C¹³-NMR spectra showed that the glucose part of curcbitacin-E-2-D-glucoside was taken away, and the structure of the aglycone did not change in any other way. ¹H-NMR spectral data of cucurbitacin-E proved that no glucose moiety signals appeared in the area between δ 5.43 and 5.76 and the presence of two trans-olefinic protons (H 23 and 24) at δ 7.3-7.4. The three-proton signal at 1.22 ppm confirmed the presence of

the 25-acetate functional group, and a new signal at 8.2 ppm was assigned to the carbon methine proton at C-24.

In addition, ¹H-NMR data was supported by C13-NMR, which proved the absence of signals for the glucose moiety between 60.28 and 102.33 ppm.

¹H-NMR of DHCE indicated that it lacked the signals of the glucose moiety as well as olefinic protons H-23 and -24. Moreover, the three carbonyl signals at 120.9, 125.6, and 173.45 ppm were assigned to C-3, C-11, and C-22, respectively. The C-22 signal's downfield shift revealed the saturation of the C23-C24 double bond [45].

The absence of the glucose moiety in all metabolites suggests that glycolysis was the first step in the biotransformation sequence, followed by secondary biotransformation (Fig. 1). *Curvularia lunata* is a well-known biocatalyst that hydroxylates a variety of steroids at various locations. However, the remarkable biotransformation only occurred on the side chain, not on the main cyclic structure of cucurbitacin [46]. Fig. (1) illustrates the possible biotransformation sequence based on the identification of these metabolites.

Following glucose cleavage with CE, reduction of the conjugation 23-24 doubly bound would produce a saturated side chain to yield DHCE.

The present study investigated the anticancer activity of DHCE against A549. Researchers investigated the anticancer potential of DHCE against different cells [47, 48].

DHCE might increase cells in the G2/M phase of the cell cycle, delaying mitosis. We achieved cell cycle arrest by downregulating the production of CDC2 and cyclin B1 proteins, which in turn dissociated the CDC2/cyclin B1 complex via GADD45 upregulation [49]. Moreover, it might suppress the levels of cyclin A2, cyclin B1, and cyclin E1, resulting in an accumulation of cells in the G1/G0 phase of the cell cycle [50].

The results of the current investigation revealed that the LD₅₀ of DHCE in mice was 930 mg/kg b.w. The main toxicological effect of DHCE in experimental mice appears to be an increase in capillary permeability, irritation of the intestinal mucosa, and a strongly increased intestinal motility. The mice die from congestion of the intestine, pancreas, liver, and kidneys. We used 1/50 and 1/20 LD₅₀ of DHCE to evaluate its lung protective activity against B[a]P-induced lung cancer in mice.

According to reports, B[a]P may be a hydrocarbon that contributes to the development of lung cancer [51].

Moreover, monitoring tumor progression to identify therapy options and responses is a common mechanism for the management of lung cancer [52].

However, chemotherapy is still the only treatment option for lung cancer. Moreover, chemotherapeutics have side effects like hemopoietic tissue damage and immunological suppression, which can make it hard to take medicine or cause the patient to stop therapy [53].

Currently, cytokines and free radical suppression, as well as antioxidant induction, are widely suggested as key strategies for protecting cells from immune suppression and external carcinogens [54]. Researchers increasingly acknowledge the beneficial effects of phytochemicals with antioxidative capabilities in cancer prevention and management, commonly known as chemoprevention [55]. Chemoprevention is now the most promising approach for significantly decreasing the occurrence of lung cancer, especially in cases of B[a]P-induced lung cancer [34].

Elevation of plasma TC and TG, as well as depletion of HDL-C, occur because of several abnormalities in physiological events during carcinogenesis. This could be caused by anorexia and malabsorption. It is an indication of chemically induced organ oxidative stress and toxicity [53-55]. This study significantly reduced HDL-C in B[a]P-stimulated mice. Furthermore, B[a]P-activated animals had higher plasma TC and TG levels, which could be attributed to lung abnormalities [54].

Prophylactic treatment with DHCE at both doses, particularly 46.5 mg/kg body weight, restored the lipid profile levels in mice. We found the therapeutic activity of DHCE on plasma TC, TG, and HDL-C to be near normal, suggesting DHCE's protective benefits against lung cancer. The effect of DHCE is more pronounced than that of tamoxifen.

B[a]P is a carcinogen that generates many free radicals. Extreme radicals react with lipids to release MDA. MDA is a reactive chemical that can interact with DNA to cause mutations and cancer [54]. Currently, B[a]P-activated mice showed a significant increase in MDA compared to the control group. The prophylactic effect of DHCE treatment in B[a]P-triggered mice diminished the status of MDA considerably. Enzymatic antioxidants (GPx and CAT) and non-enzymatic GSH can elucidate this by eradicating MDA.

Using both short-term and long-term models of inflammation, Khayyal *et al.* studied how *Iberis amara* extracts (which are high in cucurbitacins) could reduce inflammation and protect cells from damage [56]. Because cucurbitacins B, E, and I are in the extract, both models showed a decrease in inflammation that was related to the dose. This supports the idea that the extract has strong anti-inflammatory properties [57]. Our results were in line with several articles that proved the antioxidant activity of certain medicinal plants due to the presence of cucurbitacins [58, 59].

Cancer development depends in large part on chronic inflammation. Two key proteins, IL-6 and NF- κ B, regulate inflammation-related cancers. While IL-6 is a crucial component of cell development and cell variety, NF- κ B is the cause of tissue inflammation.

Similarly, MMP-2 and MMP-12 play a vital role in inflammation and are required for acute cigarette smoke-induced connective tissue breakdown [60]. A number of studies [61, 62] have also shown that cultured macrophages from the lavage fluid of human smokers or from animals exposed to smoke have higher electrolytic

activity. Human lungs with emphysema also exhibit higher levels of MMP-2 and MMP-12 than lungs without the disease [63].

The lungs of B[a]P-treated mice contained significantly more proinflammatory mediators, such as IL-6, NF- κ B, MMP-2, and MMP-12, compared to the control group. In B[a]P-induced animals, Preventive DHCE treatment returned this state to normal. This was unmistakably confirmed by histological findings that showed reduced harm in the lung alveolar, pointing to the antitumor effect of DHCE against experimental lung cancer caused by B[a]P.

DHCE's anti-inflammatory and antiproliferative effects were also caused by its role in the polymerization of the actin cytoskeleton [64]. We demonstrated that DHCE not only reduced B[a]P-induced inflammation, but also lowered the levels of IL-6, MMP-2, and MMP-12. A lower level of NF- κ B protein showed that DHCE also slowed down lung apoptosis in rats that had been given B[a]P. Furthermore, studies have reported that DHCE exhibits protective properties in a model of various diseases by regulating cytokine pathways [65]. Consequently, our study revealed that DHCE improved lung injury and attenuated inflammation impairment, including cytokine inhibition and increased antioxidant biomarkers. These results showed that DHCE improved B[a]P-induced lung cancer in mice.

In the present investigation, we observed a striking increase in inflammatory mediators as well as a decrease in the level of antioxidant biomarkers in mice treated with B[a]P. The statistical analysis and histopathological examination clearly showed that this reflects systemic inflammation.

In the current study, B[a]P administration overexpressed cPLA2, stimulating the lung cells to produce and biosynthesize arachidonic, lipoxygenases and cyclooxygenases then transferred to eicosanoids [66], including prostaglandins [67]. Eicosanoids such as the cytokines IL-6 and NF- κ B serve as chemoattractants for neutrophils, playing a key role in the inflammatory process [68] (Chart 1). In addition, the broken cell membrane moved the lung cell's released IL-6 and NF- κ B into the cytoplasm, which led to an increase in sPLA2 levels [69]. Moreover, overexpression of sPLA2 led to surfactant catabolism, oxygenation impairment, and acute respiratory distress syndrome (ARDS) [24]. Surprisingly, we discovered that DHCE lowers the expression of cPLA2 and sPLA2 in B[a]P-induced cells. This lowers the cytokine storm, which is the main cause of ARDS and lung cancer.

As a result, cancer therapy that uses apoptosis induction and cycle arrest of cancer cells is effective [70]. In this study, DHCE treatment of lung toxicity cells resulted in improvement of oxidative stress biomarkers and inflammatory mediators, typical signs of cell recovery [71]. In addition, DHCE's anti-inflammatory and anti-oxidant effects depend on the dose. It does this by decreasing the production of proapoptotic proteins and restoring normal levels of enzymatic and non-enzymatic antioxidant biomarkers.

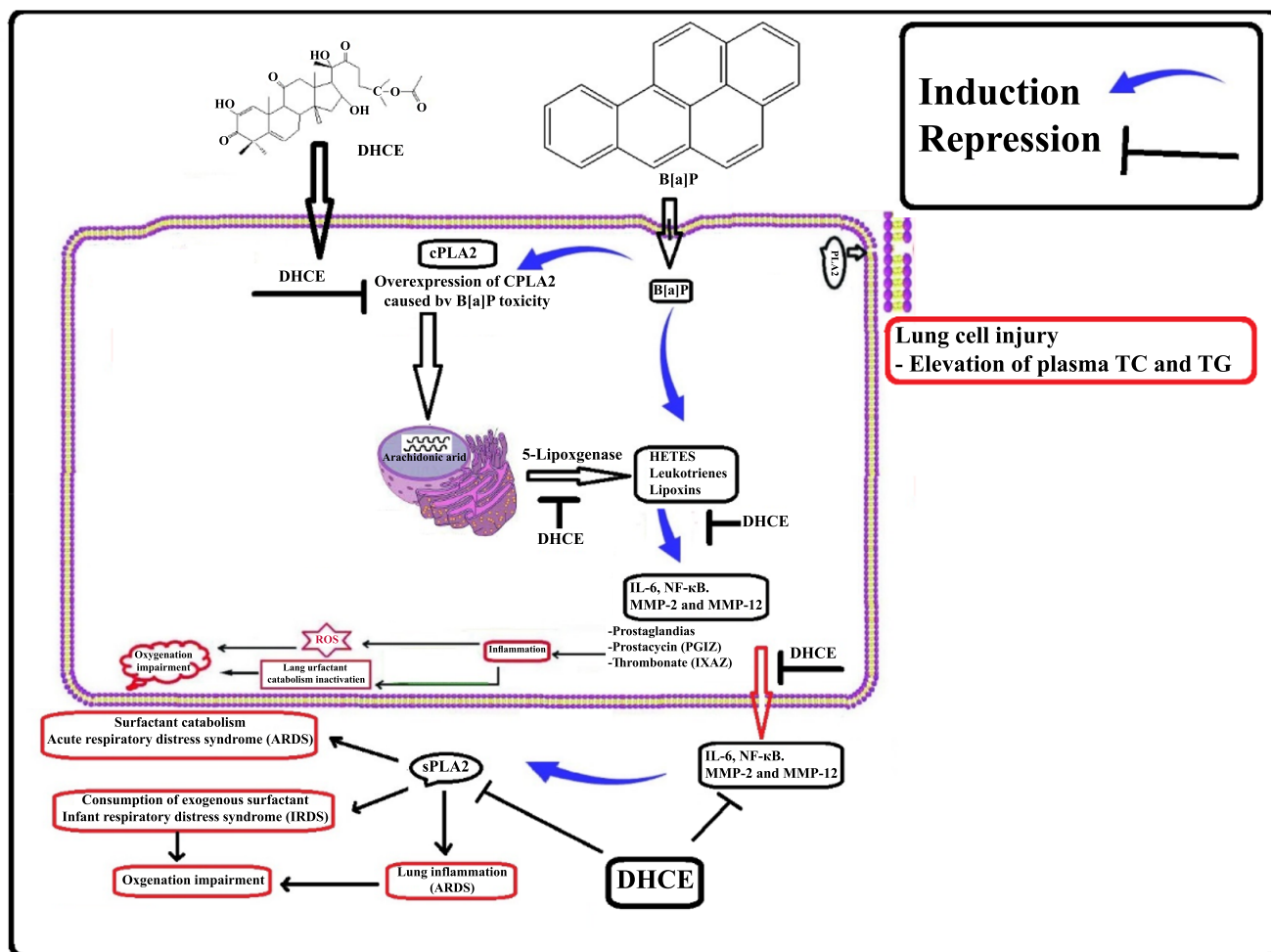


Chart (1). The perspective mechanism of action for DHCE.

Our results established the cytotoxic potential of DHEC in humans against the lung cancer cell line A549. Consistently, the administration of DHEC led to a decrease in ROS and cytokine production, as well as a downregulation of cPLA2 and sPLA2. The combined information from *in vitro* and *in vivo* research has successfully identified the advantages of DHEC in the treatment of lung cancer. An increase in antioxidant enzymes indicates the activation of intrinsic apoptosis, thereby reinforcing the cytotoxicity evidence.

The current study's histological results demonstrated that DHCE influenced the protection of the lung structure in mice suffering from lung cancer due to exposure to B[a]P. Treatment with DHCE significantly reduced the severity of toxicity and stellate infiltration compared with the B[a]P-treated control group.

Our biochemical, molecular biological, and histological results also showed that DHCE may help protect the lungs of mice from lung toxicity caused by B[a]P.

To our knowledge, DHCE, a cucurbitacin-E-glucoside

metabolite of *C. lunata* NRRL 2178 biotransformation, has never been documented as a protector against B[a]P-induced lung damage, and this investigation may be the first of its kind.

CONCLUSION

Overall, the current study on DHCE showed well measured *in vitro* and *in vivo* investigations that suggest beneficial effects on lung cancer brought on by B[a]P and inflammatory oxidative damage. Therefore, these preliminary findings suggest DHCE as a potential lung cancer chemoprevention candidate. Future studies will be necessary to clarify the potential molecular processes essential to the apparent anticancer action.

AUTHORS' CONTRIBUTION

Experimental design for the NRRL 2178 biotransformation of cucurbitacin-E-glucoside was carried out by Prof. Mahmoud Abdel-Mongy and Dr. Fotna Magdy. Prof. Tamer Roshdy and Prof. Ahmed Salah conducted *in vitro* and *in vivo* studies of the obtained metabolite, DHCE. The

biochemical study was carried out by Prof. Hussein MA. We wrote the first draft of the manuscript, managed the analyses of the study, and managed the literature searches carried out in collaboration with all authors.

LIST OF ABBREVIATIONS

| | | |
|-------|---|-----------------------------|
| DHCE | = | dihydro-cucurbitacin-E |
| TC | = | Total Cholesterol |
| GSH | = | Glutathione |
| MMP-2 | = | Matrix Metalloproteinases-2 |
| sPLA2 | = | Secretory Phospholipase A2 |
| IL-6 | = | Interleukin-6 |
| GPx | = | Glutathione Peroxidase |

ETHICS APPROVAL AND CONSENT TO PARTICIPATE

The experiment received approval from the Ethics Committee of the Faculty of Applied Health Science and Technology, Egypt (Reference number 20221025).

HUMAN AND ANIMAL RIGHTS

The animal research techniques were conducted according to the guidelines specified in the ninth edition of the Guide for the Care and Use of Laboratory Animals issued by the National Academy of Sciences, National Academies Press, Washington, D.C./ This study adheres to internationally accepted standards for animal research, following the 3Rs principle. The ARRIVE guidelines were employed for reporting experiments involving live animals, promoting ethical research practices.

CONSENT FOR PUBLICATION

Not applicable.

AVAILABILITY OF DATA AND MATERIALS

The data of current study are available from author, [M.A], on a reasonable request.

FUNDING

None.

CONFLICT OF INTEREST

The authors declare no conflict of interest, financial or otherwise.

ACKNOWLEDGEMENTS

Declared none.

REFERENCES

- [1] Lung cancer. 2023. Available from: <https://www.who.int/news-room/fact-sheets/detail/lung-cancer>
- [2] Ferlay J, Shin HR, Bray F, Forman D, Mathers C, Parkin DM. Estimates of worldwide burden of cancer in 2008: GLOBOCAN 2008. *Int J Cancer* 2010; 127(12): 2893-917. <http://dx.doi.org/10.1002/ijc.25516> PMID: 21351269
- [3] Vu AT, Taylor KM, Holman MR, Ding YS, Hearn B, Watson CH. Polycyclic aromatic hydrocarbons in the mainstream smoke of popular US cigarettes. *Chem Res Toxicol* 2015; 28(8): 1616-26.

- <http://dx.doi.org/10.1021/acs.chemrestox.5b00190> PMID: 26158771
- [4] Emara AA, Darwesh AM, Mostafa MA, *et al.* Synthesis of CEG-AgNPs as a promising MMPs/COX-2/Bcl-2 signaling pathway modulator in BaP-Induced lung carcinoma. *Asian J Chem* 2022; 34(2): 289-96. <http://dx.doi.org/10.14233/ajchem.2022.23456>
- [5] Omidian K, Rafiei H, Bandy B. Polyphenol inhibition of benzo[a]pyrene-induced oxidative stress and neoplastic transformation in an *in vitro* model of carcinogenesis. *Food Chem Toxicol* 2017; 106: 165-74. <http://dx.doi.org/10.1016/j.fct.2017.05.037> PMID: 28533128
- [6] Torkey HM, Abou-Yousef HM, Abdel Azeiz AZ, Farid H. Insecticidal effect of cucurbitacin E glycoside isolated from *Citrullus colocynthis* against *Aphis craccivora*. *Aust J Basic Appl Sci* 2009; 3: 4060-6.
- [7] Wang K, Song Z, Wang H, Li Q, Cui Z, Zhang Y. *Angelica sinensis* polysaccharide attenuates concanavalin A-induced liver injury in mice. *Int Immunopharmacol* 2016; 31: 140-8. <http://dx.doi.org/10.1016/j.intimp.2015.12.021> PMID: 26741264
- [8] Hussain AI, Rathore HA, Sattar MZA, Chatha SAS, Sarker SD, Gilani AH. *Citrullus colocynthis* (L.) Schrad (bitter apple fruit): A review of its phytochemistry, pharmacology, traditional uses and nutritional potential. *J Ethnopharmacol* 2014; 155(1): 54-66. <http://dx.doi.org/10.1016/j.jep.2014.06.011> PMID: 24936768
- [9] He S, Ou R, Wang W, *et al.* *Camptosorus sibiricus* rupestris aqueous extract prevents lung tumorigenesis via dual effects against ROS and DNA damage. *J Ethnopharmacol* 2018; 220: 44-56. <http://dx.doi.org/10.1016/j.jep.2017.12.021> PMID: 29258855
- [10] Basha SZ, Mohamed GA, Abdel-Naim AB, Hasan A, Abdel-Lateff A. Cucurbitacin E glucoside from *Citrullus colocynthis* inhibits testosterone-induced benign prostatic hyperplasia in mice. *Drug Chem Toxicol* 2021; 44(5): 533-43. <http://dx.doi.org/10.1080/01480545.2019.1635149> PMID: 31298051
- [11] Gao F, Zhang JM, Wang ZG, Peng W, Hu HL, Fu CM. Biotransformation, a promising technology for anti-cancer drug development. *Asian Pac J Cancer Prev* 2013; 14(10): 5599-608. <http://dx.doi.org/10.7314/APJCP.2013.14.10.5599> PMID: 24289549
- [12] Changtam C, Sukcharoen O, Yingyongnarongkul B, Suksamrarn A. Biotransformations of 20-hydroxyecdysone and analogues by *Curvularia lunata* NRRL 2178. *Steroids* 2006; 71(10): 902-7. <http://dx.doi.org/10.1016/j.steroids.2006.06.002> PMID: 16846623
- [13] Collins D, Reynolds WF, Reese PB. Aromadendrane transformations by *Curvularia lunata* ATCC 12017. *Phytochemistry* 2002; 60(5): 475-81. [http://dx.doi.org/10.1016/S0031-9422\(02\)00136-X](http://dx.doi.org/10.1016/S0031-9422(02)00136-X) PMID: 12052513
- [14] M Soliman S, Mosallam S, Mamdouh MA, Hussein MA, M Abd El-Halim S. Design and optimization of cranberry extract loaded bile salt augmented liposomes for targeting of MCP-1/STAT3/VEGF signaling pathway in DMN-intoxicated liver in rats. *Drug Deliv* 2022; 29(1): 427-39. <http://dx.doi.org/10.1080/10717544.2022.2032875> PMID: 35098843
- [15] Mohamad EA, Mohamed ZN, Hussein MA, Elneklawi MS. GANE can improve lung fibrosis by reducing inflammation via promoting p38MAPK/TGF- β 1/NF- κ B signaling pathway downregulation. *ACS Omega* 2022; 7(3): 3109-20. <http://dx.doi.org/10.1021/acsomega.1c06591> PMID: 35097306
- [16] Hussein MA. Synthesis of some novel triazoloquinazolines and triazinoquinazolines and their evaluation for anti-inflammatory activity. *Med Chem Res* 2012; 21(8): 1876-86. <http://dx.doi.org/10.1007/s00044-011-9707-0>
- [17] Mohammed Abdalla H Jr, Soad Mohamed AG. *In vivo* hepatoprotective properties of purslane extracts on paracetamol-induced liver damage. *Malays J Nutr* 2010; 16(1): 161-70. PMID: 22691863
- [18] Shehata MR, Mohamed MMA, Shoukry MM, Hussein MA, Hussein

- FM. Synthesis, characterization, equilibria and biological activity of dimethyltin(IV) complex with 1,4-piperazine. *J Coord Chem* 2015; 68(6): 1101-14.
<http://dx.doi.org/10.1080/00958972.2015.1007962>
- [19] Elgizawy HA, Ali AA, Hussein MA. Resveratrol: Isolation, and its nanostructured lipid carriers, inhibits cell proliferation, induces cell apoptosis in certain human cell lines carcinoma and exerts protective effect against paraquat-induced hepatotoxicity. *J Med Food* 2021; 24(1): 89-100.
<http://dx.doi.org/10.1089/jmf.2019.0286> PMID: 32580673
- [20] El-gizawy HAE, Hussein MA. Isolation, structure elucidation of ferulic and coumaric acids from *Fortunella japonica* swingle leaves and their structure antioxidant activity relationship. *Free Radic Antioxid* 2016; 7(1): 23-30.
<http://dx.doi.org/10.5530/fra.2017.1.4>
- [21] Abdel Maksoud HA, Elharrif MG, Mahfouz MK, Omnia MA, Abdullah MH, Eltabey ME. Biochemical study on occupational inhalation of benzene vapours in petrol station. *Respir Med Case Rep* 2019; 27: 100836.
<http://dx.doi.org/10.1016/j.rmcr.2019.100836> PMID: 31008048
- [22] El Gizawy HA, Abo-Salem HM, Ali AA, Hussein MA. Phenolic profiling and therapeutic potential of certain isolated compounds from *Parkia roxburghii* against AChE activity as well as GABA α 5, GSK-3 β , and p38 α MAP-Kinase Genes. *ACS Omega* 2021; 6(31): 20492-511.
<http://dx.doi.org/10.1021/acsomega.1c02340> PMID: 34395996
- [23] Hussein MA, Borik RM. A novel quinazoline-4-one derivatives as a promising cytokine inhibitors: Synthesis, molecular docking, and structure-activity relationship. *Curr Pharm Biotechnol* 2022; 23(9): 1179-203.
<http://dx.doi.org/10.2174/1389201022666210601170650> PMID: 34077343
- [24] Hussein MA, Ismail NEM, Mohamed AH, Borik RM, Ali AA, Mosaad YO. Plasma phospholipids: A promising simple biochemical parameter to evaluate COVID-19 infection severity. *Bioinform Biol Insights* 2021; 15
<http://dx.doi.org/10.1177/11779322211055891> PMID: 34840499
- [25] Boshra SA, Hussein MA. Cranberry extract as a supplemented food in treatment of oxidative stress and breast cancer induced by N-Methyl-N-Nitrosourea in female virgin rats. *Int J Phytomed* 2016; 8: 217-27.
- [26] Yuyama KT, Fortkamp D, Abraham WR. Eremophilane-type sesquiterpenes from fungi and their medicinal potential. *Biol Chem* 2017; 399(1): 13-28.
<http://dx.doi.org/10.1515/hsz-2017-0171> PMID: 28822220
- [27] Hussein MA, El-gizawy HAE, Gobba NAEK, Mosaad YO. Synthesis of cinnamyl and caffeoyl derivatives of cucurbitacin-eglycoside isolated from *Citrullus colocynthis* fruits and their structures antioxidant and anti-inflammatory activities relationship. *Curr Pharm Biotechnol* 2017; 18(8): 677-93.
<http://dx.doi.org/10.2174/1389201018666171004144615> PMID: 28982326
- [28] Mohamed GA, Ibrahim SRM, El-Agamy DS, et al. Cucurbitacin E glucoside alleviates concanavalin A-induced hepatitis through enhancing SIRT1/Nrf2/HO-1 and inhibiting NF- κ B/NLRP3 signaling pathways. *J Ethnopharmacol* 2022; 292: 115223.
<http://dx.doi.org/10.1016/j.jep.2022.115223> PMID: 35354089
- [29] Wang S, Lu Z, Lang B, Wang X, Li Y, Chen J. *Curvularia lunata* and curvularia leaf spot of maize in China. *ACS Omega* 2022; 7(51): 47462-70.
<http://dx.doi.org/10.1021/acsomega.2c03013> PMID: 36591195
- [30] Hou JM, Ma BC, Zuo YH, et al. Rapid and sensitive detection of *Curvularia lunata* associated with maize leaf spot based on its *Clg2p* gene using semi-nested PCR. *Lett Appl Microbiol* 2013; 56(4): 245-50.
<http://dx.doi.org/10.1111/lam.12040> PMID: 23278833
- [31] Lu Y, Song Y, Xue Z. Multiplex polymerase chain reaction detection of *Curvularia lunata*, *Bipolaris maydis*, and *Aureobasidium zeae* in infected maize leaf tissues. *J Basic Microbiol* 2019; 59(9): 862-6.
<http://dx.doi.org/10.1002/jobm.201900185> PMID: 31330054
- [32] van de Loosdrecht AA, Beelen RH, Ossenkoppele GJ, Broekhoven MG, Langenhuijsen MM. A tetrazolium-based colorimetric MTT assay to quantitate human monocyte mediated cytotoxicity against leukemic cells from cell lines and patients with acute myeloid leukemia. *J Immunol Methods* 1994; 174(1-2): 311-20.
[http://dx.doi.org/10.1016/0022-1759\(94\)90034-5](http://dx.doi.org/10.1016/0022-1759(94)90034-5)
- [33] Abal P, Louzao M, Antelo A, et al. Acute oral toxicity of tetrodotoxin in mice: Determination of lethal dose 50 (LD50) and no observed adverse effect level (NOAEL). *Toxins (Basel)* 2017; 9(3): 75.
<http://dx.doi.org/10.3390/toxins9030075> PMID: 28245573
- [34] Elsheikh AM, M Roshdy T, Hassan SA, A Hussein M, M Fayed A. Resveratrol: A potential protector against benzo[a]pyrene-induced lung toxicity. *Pak J Biol Sci* 2022; 25(1): 78-89.
<http://dx.doi.org/10.3923/pjbs.2022.78.89> PMID: 35001578
- [35] Kim CS, Choi SJ, Park CY, Li C, Choi JS. Effects of silybinin on the pharmacokinetics of tamoxifen and its active metabolite, 4-hydroxytamoxifen in rats. *Anticancer Res* 2010; 30(1): 79-85. PMID: 20150620
- [36] Fossati P, Prencipe L. Serum triglycerides determined colorimetrically with an enzyme that produces hydrogen peroxide. *Clin Chem* 1982; 28(10): 2077-80.
<http://dx.doi.org/10.1093/clinchem/28.10.2077> PMID: 6812986
- [37] Allain CC, Poon LS, Chan CSG, Richmond W, Fu PC. Enzymatic determination of total serum cholesterol. *Clin Chem* 1974; 20(4): 470-5.
<http://dx.doi.org/10.1093/clinchem/20.4.470> PMID: 4818200
- [38] Gao B, Saralamba S, Lubell Y, White L, Dondorp AM, Aguas R. Determinants of MDA impact and designing MDAs towards malaria elimination. *Elife* 2020; 9: e51773.
<http://dx.doi.org/10.7554/eLife.51773>
- [39] Burstein M, Scholnick HR, Morfin R. Rapid method for the isolation of lipoproteins from human serum by precipitation with polyanions. *J Lipid Res* 1970; 11(6): 583-95.
[http://dx.doi.org/10.1016/S0022-2275\(20\)42943-8](http://dx.doi.org/10.1016/S0022-2275(20)42943-8) PMID: 4100998
- [40] Bancroft GD, Steven A. Theory and Practice of Histological Technique. New York: Churchill Livingstone 1983; pp. 99-112.
- [41] Petronelli A, Pannitteri G, Testa U. Triterpenoids as new promising anticancer drugs. *Anticancer Drugs* 2009; 20(10): 880-92.
<http://dx.doi.org/10.1097/CAD.0b013e328330fd90> PMID: 19745720
- [42] Garcia-Granados A, Martinez A, Parra A, Rivas F. Manoyl-oxide biotransformations with filamentous fungi. *Curr Org Chem* 2007; 11(8): 679-92.
<http://dx.doi.org/10.2174/138527207780598774>
- [43] Arantes S, Hanson J. The biotransformation of sesquiterpenoids by *Mucor plumbeus*. *Curr Org Chem* 2007; 11(8): 657-63.
<http://dx.doi.org/10.2174/138527207780598747>
- [44] Parra A, Rivas F, Garcia-Granados A, Martinez A. Microbial transformation of triterpenoids. *Mini Rev Org Chem* 2009; 6(4): 307-20.
<http://dx.doi.org/10.2174/157019309789371569>
- [45] Mohapatra RK, Perekhoda L, Azam M, et al. Computational investigations of three main drugs and their comparison with synthesized compounds as potent inhibitors of SARS-CoV-2 main protease (M^{pro}): DFT, QSAR, molecular docking, and *in silico* toxicity analysis. *J King Saud Univ Sci* 2021; 33(2): 101315.
<http://dx.doi.org/10.1016/j.jksus.2020.101315> PMID: 33390681
- [46] Changtam C, Sukcharoen O, Yingyongnarongkul B, Chimnoi N, Suksamrarn A. Functional group-mediated biotransformation by *Curvularia lunata* NRRL 2178: Synthesis of 3-dehydro-2-deoxyecdysteroids from the 3-hydroxy-2-mesyloxy analogues. *Tetrahedron* 2008; 64(11): 2626-33.
<http://dx.doi.org/10.1016/j.tet.2008.01.033>
- [47] Tang Y, Li W, Cao J, Li W, Zhao Y. Bioassay-guided isolation and identification of cytotoxic compounds from *Bolbostemma paniculatum*. *J Ethnopharmacol* 2015; 169: 18-23.

- <http://dx.doi.org/10.1016/j.jep.2015.04.003> PMID: 25882313
- [48] Jiang H, Tan R, Jiao R, Deng X, Tan R. Herpecaudin from *Herpetospermum caudigerum*, a xanthine oxidase inhibitor with a novel isoprenoid scaffold. *Planta Med* 2016; 82(11/12): 1122-7. <http://dx.doi.org/10.1055/s-0042-108210> PMID: 27272398
- [49] Cheng AC, Hsu YC, Tsai CC. The effects of cucurbitacin E on GADD45 β -trigger G2/M arrest and JNK-independent pathway in brain cancer cells. *J Cell Mol Med* 2019; 23(5): 3512-9. <http://dx.doi.org/10.1111/jcmm.14250> PMID: 30912292
- [50] Hsu Y-C, Chen M-J, Huang T-Y. Inducement of mitosis delay by cucurbitacin E, a novel tetracyclic triterpene from climbing stem of *Cucumis melo* L., through GADD45 γ in human brain malignant glioma (GBM) 8401 cells. *Cell Death Dis* 2014; 5(2): e1087. <http://dx.doi.org/10.1038/cddis.2014.22> PMID: 24577085
- [51] Field RW, Withers BL. Occupational and environmental causes of lung cancer. *Clin Chest Med* 2012; 33(4): 681-703. <http://dx.doi.org/10.1016/j.ccm.2012.07.001> PMID: 23153609
- [52] Farbicka P, Nowicki A. Reviews palliative care in patients with lung cancer. *Contemp Oncol (Pozn)* 2013; 3(3): 238-45. <http://dx.doi.org/10.5114/wo.2013.35033> PMID: 24596508
- [53] Dawson SJ, Tsui DWY, Murtaza M, *et al.* Analysis of circulating tumor DNA to monitor metastatic breast cancer. *N Engl J Med* 2013; 368(13): 1199-209. <http://dx.doi.org/10.1056/NEJMoa1213261> PMID: 23484797
- [54] Hussein DA, Abuelkasem MA, Hassan SS. *Salvia officinalis* improves glucose uptake and suppresses ectopic lipid deposition in obese rats with metabolic syndrome. *Curr Pharm Biotechnol* 2023. <http://dx.doi.org/10.2174/1389201024666230811104740>
- [55] Mosaad YO, Hussein MA, Ateyya H, *et al.* BAAE-AgNPs improve symptoms of diabetes in STZ-induced diabetic rats. *Curr Pharm Biotechnol* 2023; 24(14): 1812-26. <http://dx.doi.org/10.2174/1389201024666230313105049> PMID: 36915989
- [56] Khayyal M, Agha A, Zaki H, El-Sahar A, Abdel-Aziz H. Mechanisms involved in the anti-inflammatory and vascular effects of *Iberis amara* extract. *Planta Med* 2015; 81(12/13): 1097-102. <http://dx.doi.org/10.1055/s-0035-1546244> PMID: 26287692
- [57] Dong L, Almeida A, Pollier J, *et al.* An independent evolutionary origin for insect deterrent cucurbitacins in *Iberis amara*. *Mol Biol Evol* 2021; 38(11): 4659-73. <http://dx.doi.org/10.1093/molbev/msab213> PMID: 34264303
- [58] Delporte C, Muñoz O, Rojas J, *et al.* Pharmacotoxicological study of *Kageneckia oblonga*, Rosaceae. *Z Naturforsch C J Biosci* 2002; 57(1-2): 100-8. <http://dx.doi.org/10.1515/znc-2002-1-218> PMID: 11926521
- [59] Wan J, Wang XJ, Guo N, *et al.* Highly oxygenated triterpenoids and diterpenoids from Fructus Rubi (*Rubus chingii* Hu) and their NF- κ B inhibitory effects. *Molecules* 2021; 26(7): 1911-21. <http://dx.doi.org/10.3390/molecules26071911> PMID: 33805414
- [60] Liu L, Guo H, Song A, *et al.* Progranulin inhibits LPS-induced macrophage M1 polarization via NF- κ B and MAPK pathways. *BMC Immunol* 2020; 21(1): 32. <http://dx.doi.org/10.1186/s12865-020-00355-y> PMID: 32503416
- [61] Ozeki N, Kawai R, Yamaguchi H, *et al.* RETRACTED: IL-1 β -induced matrix metalloproteinase-13 is activated by a disintegrin and metalloprotease-28-regulated proliferation of human osteoblast-like cells. *Exp Cell Res* 2014; 323(1): 165-77. <http://dx.doi.org/10.1016/j.yexcr.2014.02.018> PMID: 24613731
- [62] Joos L, He JQ, Shepherdson MB, *et al.* The role of matrix metalloproteinase polymorphisms in the rate of decline in lung function. *Hum Mol Genet* 2002; 11(5): 569-76. <http://dx.doi.org/10.1093/hmg/11.5.569> PMID: 11875051
- [63] Jiang Y, Gong Q, Huang J, *et al.* ADAM-10 regulates MMP-12 during lipopolysaccharide-induced inflammatory response in macrophages. *J Immunol Res* 2022; 2022: 1-16. <http://dx.doi.org/10.1155/2022/3012218> PMID: 36157882
- [64] Sørensen PM, Iacob RE, Fritzsche M, *et al.* The natural product cucurbitacin E inhibits depolymerization of actin filaments. *ACS Chem Biol* 2012; 7(9): 1502-8. <http://dx.doi.org/10.1021/cb300254s> PMID: 22724897
- [65] Arel-Dubeau AM, Longpré F, Bournival J, *et al.* Cucurbitacin E has neuroprotective properties and autophagic modulating activities on dopaminergic neurons. *Oxid Med Cell Longev* 2014; 2014: 1-15. <http://dx.doi.org/10.1155/2014/425496> PMID: 25574337
- [66] Schaloske RH, Dennis EA. The phospholipase A2 superfamily and its group numbering system. *Biochim Biophys Acta Mol Cell Biol Lipids* 2006; 1761(11): 1246-59. <http://dx.doi.org/10.1016/j.bbalip.2006.07.011> PMID: 16973413
- [67] Serhan CN. Resolution phase of inflammation: Novel endogenous anti-inflammatory and proresolving lipid mediators and pathways. *Annu Rev Immunol* 2007; 25(1): 101-37. <http://dx.doi.org/10.1146/annurev.immunol.25.022106.141647> PMID: 17090225
- [68] Vancheri C, Mastruzzo C, Sortino MA, Crimi N. The lung as a privileged site for the beneficial actions of PGE2. *Trends Immunol* 2004; 25(1): 40-6. <http://dx.doi.org/10.1016/j.it.2003.11.001> PMID: 14698283
- [69] Hussein MA. Administration of exogenous surfactant and cytosolic phospholipase A2 α inhibitors may help COVID-19 infected patients with chronic diseases. 2021. <http://dx.doi.org/10.2174/2666796702666210311123323>
- [70] Zhang X, Qin Y, Pan Z, *et al.* Cannabidiol induces cell cycle arrest and cell apoptosis in human gastric cancer SGC-7901 cells. *Biomolecules* 2019; 9(8): 302. <http://dx.doi.org/10.3390/biom9080302>.
- [71] Yin GH, Gao FC, Tian J, *et al.* Hsa_circ_101882 promotes migration and invasion of gastric cancer cells by regulating EMT. *J Clin Lab Anal* 2019; 33(9): e23002. <http://dx.doi.org/10.1002/jcla.23002>.